Electric Field Dependence of Phase Equilibria of Binary Stockmayer Fluid Mixtures

Andras Gabor, Istvan Szalai

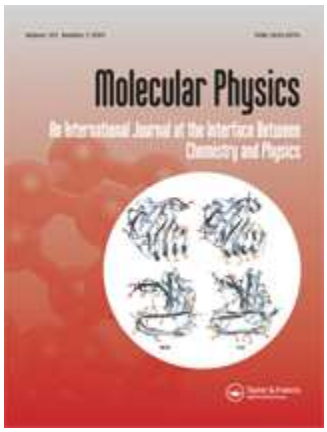

Electric Field Dependence of Phase Equilibria of Binary Stockmayer Fluid Mixtures

Journal:	*Molecular Physics*
Manuscript ID:	TMPH-2008-0002
Manuscript Type:	Full Paper
Date Submitted by the Author:	02-Jan-2008
Complete List of Authors:	Gabor, Andras; University of Pannonia, Institute of Physics Szalai, Istvan; University of Pannonia, Institute of Physics
Keywords:	perturbation theory, Stockmayer mixture, fluid-fluid equilibria
Note: The following files were submitted by the author for peer review, but cannot be converted to PDF. You must view these files (e.g. movies) online.	
gabor_molphys.tex	

Electric Field Dependence of Phase Equilibria of Binary Stockmayer Fluid Mixtures

András Gábor* and István Szalai†

Institute of Physics, University of Pannonia,

H-8201 Veszprém, P.O.Box 158, Hungary

Abstract

A perturbation theory based study of the effect of an external electric field on the phase equilibrium properties of binary Stockmayer fluids is presented. The dipole–dipole interaction and the applied field are treated as independent perturbations to a Lennard-Jones mixture, and the reference fluid is treated by the van der Waals 1-fluid approximation. A third-order free energy expression in the electric field strength is established, and the dielectric constant is calculated for a needle shaped sample parallel to the field direction. We present and discuss vapor–liquid and liquid–liquid equilibrium curves at a given temperature for some dipolar mixtures exposed to an electric field, including chlorodifluoromethane+difluoromethane and acetonitrile+methanol. A sufficiently high electric field may result in massive shifts of vapour pressures and critical or azeotropic points, and can considerably alter the properties of coexisting phases. The vapor pressure decreases with increasing field strength.

PACS numbers: 61.20.Gy, 77.22.Ch, 64.70.Fx, 64.70.Ja

*Corresponding author; Electronic address: agabor@almos.vein.hu

†Electronic address: szalai@almos.vein.hu

I. INTRODUCTION

The need to explore the changes that dipolar fluids undergo in the presence of an external electric/magnetic field stimulates both theoretical [1–4] and experimental [5, 6] research activities. Nevertheless, there is no applicable theoretical model for the more complex case of dipolar fluid mixtures in an applied electric field. In this study we propose a theory confining the treatment to binary Stockmayer fluids, and test it for several examples.

There are a lot of different methods (see Refs. [7, 8] for a review) for the calculation of thermal properties of dipolar fluid mixtures, even if we restrict the question to the vapor–liquid and liquid–liquid equilibria [9]. Among them, perturbation theory is quite adequate to determine the main effect caused by the dipole–dipole interaction on one hand, and by the electric field on the other. To be more precise, we have to apply two different perturbation theories successively. First, the dipole–dipole interaction term is determined by a functional Taylor expansion [10] of the free energy of the dipolar mixture around a nonpolar reference system. Second, we apply a so-called algebraic method [11–13] to handle the influence of an electric field. (It should be noted that the two perturbations applied one after the other act independently, and do not lead to a quadratic growth in the error of the thermodynamic quantities.) It is needless to bother too much looking for an adequate dipolar fluid model. The Stockmayer (STM) potential model where molecules have simple static, pointlike dipoles serves well for our current purposes – the polarization effect may be the subject of a subsequent study. In a more sophisticated model we would have to find a suitable reference system with known free energy, correlation functions, etc.—a serious problem of perturbation theories. In the STM model the thoroughly studied [14] Lennard-Jones fluid plays this role. Henceforth, with a free energy formula in hand the equilibrium pressure and

the corresponding mole fractions of two coexisting fluid phases can be determined by simple thermodynamical relations, and one can draw vaporisation and condensation curves for the dipolar mixture under consideration in presence of an electric field.

The outline of our paper is as follows. First of all, in Sec. II we summarise the perturbation theory for STM fluid mixtures, and the van der Waals 1-fluid approximation is applied to handle the problem of reference mixture. Then we determine the free energy of the dipolar mixture up to the third order in the applied electric field. The free energy formula (20) and the corresponding expression (22) for the dielectric constant of a needle shaped sample parallel to the field direction constitute our main theoretical results. Sec. III contains some applications of the theory. The change in the phase boundary curves as a function of the electric field strength is examined in four cases. We analyse in detail two examples for (A) vapor–liquid, and for (B) liquid–liquid equilibrium, and two real mixtures, namely (C) chlorodifluoromethane+difluoromethane, and (D) acetonitrile+methanol. In the last section, we draw some conclusions. The basic formulas of the algebraic perturbation theory for dipolar mixtures are collected in the Appendix.

II. THEORY

A. Perturbation theory for dipolar mixtures

The thermodynamical functions of STM mixtures (or even much simpler systems) can not be expressed in a closed and mathematically exact form [7], due to the multidimensional integration appearing in the partition function. However, the perturbation theory discussed below may serve a solution—at least an approximate free energy expression—if we give up the unattainable exactness.

Let us consider a fluid mixture consisting of K different species of Lennard-Jones (LJ) particles with point dipoles of magnitude $d_1, \ldots, d_K$. The ith particle of the mixture is described by the triplet $(\mathbf{r}_i, \omega_i, a_i)$ of position $\mathbf{r}_i$, orientation $\omega_i = (\phi_i \theta_i)$ given by the polar angles of the dipole moment, and of type $a_i \in \{1, \ldots, K\}$. The x_{a_i} stands for the mole fraction of species a_i. We use the LJ mixture as a reference system and a dipole–dipole interaction potential $u_{\mathrm{dd}}(ij)$ as the perturbation term. Here and in the following i stands for the triplet $(\mathbf{r}_i, \omega_i, a_i)$. The pair correlation function $g_{\mathrm{LJ}}(r_{12}, a_1 a_2)$ of the LJ mixture depends not only on the distance $r_{12} = |\mathbf{r}_1 - \mathbf{r}_2|$ of the selected particles, but on their types a_1, a_2 as well. We usually omit to note the temperature and density dependence of g_{LJ} to make our equations shorter.

In principle, the method of functional Taylor expansion around a suitably chosen reference system [10] is capable to express the free energy and the correlation functions of a fluid mixture in a power series form. For STM mixtures the third-order free energy expansion is

$$A_{\mathrm{STM}} = A_{\mathrm{LJ}} + A_1 + A_2 + A_3, \tag{1}$$

where $A_1 = 0$ due to the properties of dipole–dipole interaction, and

$$\begin{aligned} A_2 &= -\frac{4\pi}{6}\rho^2 V\beta \sum_{a_1,a_2=1}^{K} x_{a_1}x_{a_2}(d_{a_1}d_{a_2})^2 J(T,\rho,a_1a_2), \\ A_3 &= \frac{8\pi^2}{27}\rho^3 V\beta^2 \sum_{a_1,a_2,a_3=1}^{K} x_{a_1}x_{a_2}x_{a_3}(d_{a_1}d_{a_2}d_{a_3})^2 \\ &\quad \times K(T,\rho,a_1a_2a_3). \end{aligned} \tag{2}$$

See [10] for further details. In Eq. (2), $\rho = N/V$ is the number density, V is the volume of the system and $\beta = 1/k_B T$ is the inverse temperature with k_B being the Boltzmann constant.

The functions J and K are known from the literature [15], and given by the expressions

$$J(T,\rho,a_1a_2) \;=\; \int_0^\infty \mathrm{d}r_{12}\frac{1}{r_{12}^4}g_{\mathrm{LJ}}(r_{12},a_1a_2), \tag{3}$$

and

$$K(T,\rho,a_1a_2a_3) = 4\int_0^\infty \mathrm{d}r_{12}\int_0^\infty \mathrm{d}r_{13}\int_{-1}^1 \mathrm{d}(\cos\alpha_1) \times\frac{g_{\mathrm{LJ}}(r_{12},r_{13},r_{23},a_1a_2a_3)}{r_{12}r_{13}r_{23}^3}(1+3\cos\alpha_1\cos\alpha_2\cos\alpha_3), \tag{4}$$

both of which now depend on the types of the interacting particles. In Eq. (4) α_1, α_2 and α_3 denote internal angles of a triangle formed by the three molecules. The integrals (3) and (4) can only be evaluated with some simplifying assumptions. For the triplet LJ correlation function the Kirkwood superposition approximation

$$g_{\mathrm{LJ}}(r_{12},r_{13},r_{23},a_1a_2a_3) = g_{\mathrm{LJ}}(r_{12},a_1a_2)g_{\mathrm{LJ}}(r_{13},a_1a_3)g_{\mathrm{LJ}}(r_{23},a_2a_3) \tag{5}$$

is used. The additional, more severe assumptions are treated in the next section.

B. Van der Waals 1-fluid theory

The LJ pair correlation function and the free energy is not known exactly even for pure fluids to say nothing of mixtures. To surmount this problem we use the van der Waals 1-fluid (vdW1f) approximation restricting the treatment to binary fluids, and the question of reference system is solved by applying the LJ equation of state proposed by Johnson *et al.* [14]. This paper contains the most accurate values of the 33 parameters of the widely

used modified Benedict–Webb–Rubin equation of state applied first by Nicolas *et al.* [16] to the LJ fluid.

First of all, we recall briefly the vdW1f theory used for LJ mixtures (see e.g. [17, 18]). Consider a binary mixture with LJ pair potentials

$$u_{\mathrm{LJ}}(r_{12}, a_1 a_2) = 4\varepsilon_{a_1 a_2}\left[\left(\frac{\sigma_{a_1 a_2}}{r_{12}}\right)^{12} - \left(\frac{\sigma_{a_1 a_2}}{r_{12}}\right)^{6}\right]. \tag{6}$$

Here $\varepsilon_{a_1 a_2}$ and $\sigma_{a_1 a_2}$ are the energy and size parameters of the interaction of type a_1 and a_2 particles. The vdW1f theory is a conformal solution theory in which the real mixture is replaced by a hypothetical pure LJ fluid with parameters

$$\sigma_x^3 = \sum_{a_1 a_2} x_{a_1} x_{a_2} \sigma_{a_1 a_2}^3 \tag{7}$$

and

$$\varepsilon_x = \frac{1}{\sigma_x^3} \sum_{a_1 a_2} x_{a_1} x_{a_2} \varepsilon_{a_1 a_2} \sigma_{a_1 a_2}^3. \tag{8}$$

The interaction between the unlike particles of our binary mixture is described by the Lorentz–Berthelot combining rules

$$\sigma_{12} = \frac{\sigma_{11} + \sigma_{22}}{2}, \qquad \varepsilon_{12} = \sqrt{\varepsilon_{11}\varepsilon_{22}} \tag{9}$$

as the standard choice.

Let us introduce the reduced temperature, density and dipole moment by

$$T^* = \frac{k_B T}{\varepsilon_x}, \qquad \rho^* = \rho\sigma_x^3, \qquad {d_a^*}^2 = \frac{{d_a}^2}{\varepsilon_x \sigma_x^3}. \tag{10}$$

Now the pair correlation function $g_{\mathrm{LJ}}(r_{12}, a_1 a_2)$ turns into $g_{\mathrm{LJ}}(r_{12}^*)$ where $r_{12}^* = r_{12}/\sigma_x$, and dividing the integrals (3) and (4) by σ_x^3 we obtain

$$J(T^*, \rho^*) \; = \; \int_0^\infty \mathrm{d}r_{12}^* \frac{1}{r_{12}^{*4}} g_{\mathrm{LJ}}(r_{12}^*) \tag{11}$$

and

$$\begin{aligned} K(T^*, \rho^*) = 4 \int_0^\infty \mathrm{d}r_{12}^* \int_0^\infty \mathrm{d}r_{13}^* \int_{-1}^1 \mathrm{d}(\cos\alpha_1) \\ \times \frac{g_{\mathrm{LJ}}(r_{12}^*) g_{\mathrm{LJ}}(r_{13}^*) g_{\mathrm{LJ}}(r_{23}^*)}{r_{12}^* r_{13}^* r_{23}^{*3}} (1 + 3\cos\alpha_1 \cos\alpha_2 \cos\alpha_3), \end{aligned} \tag{12}$$

which depend only on the parameters of a pure (although hypothetical) fluid. In our calculations for the J and K integrals we used the formulae of Luckas *et al.* [15]. With the notation introduced above the reduced free energy $A_{\mathrm{STM}}^* = A_{\mathrm{STM}}/N\varepsilon_x$ with the usual Padé approximation is

$$A_{\mathrm{STM}}^* = A_{\mathrm{LJ}}^* + \frac{A_2^*}{1 - A_3^*/A_2^*}, \tag{13}$$

where A_{LJ}^* is taken from Ref. [14]. The second and third-order reduced free energy terms

are

$$A_2^* = -\frac{27}{8\pi}\frac{T^*}{\rho^*}y^2 J(T^*,\rho^*),$$
$$A_3^* = \frac{27}{8\pi}\frac{T^*}{\rho^*}y^3 K(T^*,\rho^*), \tag{14}$$

where

$$y = \frac{4\pi}{9}\frac{\rho^*}{T^*}\sum_a x_a d_a^{*2} \tag{15}$$

is the dipole strength function of the mixture.

C. The case of an external field

Let the Stockmayer mixture exposed to a weak homogenous electric field $\mathbf{E}_{\text{ext}} = E_{\text{ext}}\mathbf{e}_z$. The algebraic perturbation theory (summarised in the Appendix) is applied to describe the free energy contributions due to the interaction of dipoles with the electric field. Following the symbolism introduced in the Appendix the effect of the external field on the ith particle (characterised by $(\mathbf{r}_i, \phi_i\theta_i, a_i)$) is

$$u^1(i) = -E_{\text{ext}} d_{a_i} \cos\theta_i,$$

and the corresponding Mayer function turns to

$$f_{\text{M}}(i) = \exp\left(\beta E_{\text{ext}} d_{a_i} \cos\theta_i\right) - 1. \tag{16}$$

The series expansion derived to the free energy of the STM mixture in external field is:

$$A = A_{\mathrm{STM}} - \frac{1}{\beta}\frac{\rho}{4\pi}q_1 - \frac{1}{2\beta}\left(\frac{\rho}{4\pi}\right)^2 q_2 - \ldots, \tag{17}$$

where the coefficients q_i are given by (A.15). A straightforward calculation (see Refs. [12, 13]) up to third order in E_{ext} leads to

$$\begin{aligned} q_1 &= V\frac{4\pi\beta^2}{6}\sum_{a_1} x_{a_1} d_{a_1}^2 E_{\mathrm{ext}}^2, \\ q_2 &= V\frac{(4\pi\beta)^3}{27}\sum_{a_1 a_2} x_{a_1} x_{a_2} (d_{a_1} d_{a_2})^2 E_{\mathrm{ext}}^2 \\ &- \rho V\frac{(4\pi\beta)^4}{243}\sum_{a_1 a_2 a_3} x_{a_1} x_{a_2} x_{a_3} (d_{a_1} d_{a_2} d_{a_3})^2 E_{\mathrm{ext}}^2 \\ &+ \rho V\frac{(4\pi\beta)^4}{27}\sum_{a_1 a_2 a_3} x_{a_1} x_{a_2} x_{a_3} (d_{a_1} d_{a_2} d_{a_3})^2 E_{\mathrm{ext}}^2 \\ &\times L(T, \rho, a_1 a_2 a_3). \end{aligned} \tag{18}$$

Here the function L is introduced by

$$\begin{aligned} L(T, \rho, a_1 a_2 a_3) &= \frac{1}{2}\int_0^\infty \mathrm{d}r_{12} \int_0^\infty \mathrm{d}r_{13} \int_{-1}^1 \mathrm{d}(\cos\alpha_1) \\ &\times \frac{g_{\mathrm{LJ}}(r_{12} r_{13} r_{23}, a_1 a_2 a_3)}{r_{12} r_{13}} (3\cos^2\alpha_1 - 1). \end{aligned} \tag{19}$$

The three-particle correlation function of the LJ mixture appeared anew which we can only handle with the Kirkwood approximation (5) and vdW1f theory restricting the treatment to binary fluids. In the vdW1f approximation, for the reduced free energy $A^* = A/N\varepsilon_x$

of a binary STM fluid exposed to an external field we find that

$$A^* = A^*_{\rm STM} - \frac{3}{8\pi}\frac{E^{*2}_{\rm ext}}{\rho^*}\left(y + y^2 - y^3 + 9y^3 L(T^*, \rho^*)\right). \tag{20}$$

Here $E^{*2}_{\rm ext} = E^2_{\rm ext}\sigma_x^3/\varepsilon_x$ and the function $L(T^*, \rho^*)$ is given in the next section.

From the free energy we can easily derive the polarization

$$\mathbf{P} = -\frac{1}{V}\left(\frac{\partial A}{\partial \mathbf{E}_{\rm ext}}\right)_{V,T,\{x_a\}}.$$

The resulting equation is:

$$\mathbf{P} = -\frac{3}{4\pi}\left(y + y^2 - y^3 + 9y^3 L(T^*, \rho^*)\right)\mathbf{E}_{\rm ext}. \tag{21}$$

For a needle-shaped sample (parallel to the z-axis) the field strength inside the fluid is identical [12, 19] to the external field $\mathbf{E}_{\rm ext}$ and $4\pi\mathbf{P} = (\epsilon - 1)\mathbf{E}_{\rm ext}$, therefore the dielectric constant reads as

$$\epsilon = 1 + 3y + 3y^2 - 3y^3 + 27y^3 L(T^*, \rho^*). \tag{22}$$

Equation (22) looks like the corresponding formula given in Ref. [20] for the dielectric constant of dipolar hard sphere fluids (see also Ref. [12]), which expression proved to be quite accurate up to moderately high dipole moments. But, now both the dipole strength function y and $L(T^*, \rho^*)$ are complicated functions of the fluid parameters of the *mixture*.

D. Determination of the function $L(T^*, \rho^*)$

In the vdW1f approximation, the function L defined by Eq. (19) (originating from the application of the algebraic method to the STM mixture exposed to an external field) simplifies to

$$L(T^*, \rho^*) = \frac{1}{2} \int_0^\infty \mathrm{d}r_{12}^* \int_0^\infty \mathrm{d}r_{13}^* \int_{-1}^1 \mathrm{d}(\cos\alpha_1) \times \frac{g_{\mathrm{LJ}}(r_{12}^*) g_{\mathrm{LJ}}(r_{13}^*) g_{\mathrm{LJ}}(r_{23}^*)}{r_{12}^* r_{13}^*} (3\cos^2\alpha_1 - 1). \quad (23)$$

The function $L(T^*, \rho^*)$ is well known [20] for hard sphere fluids (where it does not depend on T^*, of course), and examined thoroughly by Goldman [21] for LJ fluids. The two main methods described in the literature for the calculation of $L(T^*, \rho^*)$ are the hat-function method [22] and a method based on Fourier transforms and the convolution theorem (see [21] and the references therein). Goldman's paper contains $L(T^*, \rho^*)$ in tabular form for the ranges $0.6 \leq \rho^* \leq 1.0$ and $0.6 \leq T^* \leq 4.0$, but we could not find any data for low densities in the literature. Our intended phase equilibrium investigations, however, require to fill this gap.

Our calculations confirmed that the two methods give essentially identical results at high densities [21], but the hat-function method proved to be more adequate at low densities. Going into details, a 'hatted' function

$$\hat{f}(r^*) = \frac{g_{\mathrm{LJ}}(r^*)}{r^{*3}} - 3 \int_{r^*}^\infty \mathrm{d}x \frac{g_{\mathrm{LJ}}(x)}{x^4} \quad (24)$$

has been introduced in Ref. [22] to transform (23) into a short-ranged integral

$$L(T^*,\rho^*) = \int_0^\infty \mathrm{d}r_{12}^* r_{12}^* g_{\mathrm{LJ}}(r_{12}^*) \int_0^\infty \mathrm{d}r_{13}^* r_{13}^* \hat{f}(r_{13}^*) \times \int_{|r_{12}^*-r_{13}^*|}^{|r_{12}^*+r_{13}^*|} \mathrm{d}r_{23}^* r_{23}^* \hat{f}(r_{23}^*). \quad (25)$$

We applied the simple trapezoidal integration rule in Eq. (25), and the pair correlation function $g_{\mathrm{LJ}}(r_{12}^*)$ was taken from Monte Carlo (MC) simulations performed with 512 LJ particles. The simulations were started from a randomly generated configuration and the first 15 000 MC cycles were thrown away. The length of the production period was 30 000 000 moves with acceptance ratio $40\% - 60\%$. The half of the boxlength was divided into 400 'bins' and the resulting histogram was used for the calculation of the pair correlation function, likewise in Ref. [23]. The low density limit of $L(T^*,\rho^*)$ can be given by the cluster expansion [7]

$$g_{\mathrm{LJ}}(\rho^*, r_{12}^*) = \exp\left(-\beta u_{\mathrm{LJ}}(r_{12}^*)\right) + O(\rho^*) \quad (26)$$

of the pair correlation function. We kept in Eq. (26) the first term only, and we extended the MC simulation data with the resulting $L(T^*,\rho^* \approx 0)$ values. Finally, the following interpolation equation [15] was fitted to our approximately 270 data points taken from the ranges $0.0 \le \rho^* \le 0.9$ and $0.7 \le T^* \le 3.0$:

$$L(T^*,\rho^*) = B_1 + B_2 T^* + B_3 \exp\frac{4}{T^*}\left(1 - \frac{\rho^*}{\sqrt{2}}\right) + B_4 \exp\frac{3}{T^*}\left(1 - \frac{\rho^*}{\sqrt{2}}\right), \quad (27)$$

where

$$B_j = b_{1j} + b_{2j}\rho^* + b_{3j}\rho^{*2} + b_{4j}\rho^{*3}.$$

The coefficients b_{ij} are displayed in Table I.

III. APPLICATIONS

Our aim is to study the influence of the electric field on the phase equilibria of binary STM fluids. Two phases (either vapor and liquid or two liquids) marked by prime and double-prime are in equilibrium at a common temperature T if [8]

$$\begin{aligned} p'(\rho', x_1') &= p''(\rho'', x_1''), \\ \mu_1'(\rho', x_1') &= \mu_1''(\rho'', x_1''), \\ \mu_2'(\rho', x_1') &= \mu_2''(\rho'', x_1''), \end{aligned} \tag{28}$$

where p is the pressure and μ_i is the chemical potential of the ith component in the corresponding phases. In both phases the density and the mole fraction of the 1st fluid component (x_1) are chosen as independent variables. For the binary systems studied in this paper the reduced pressure and chemical potentials of the components are derived from our free energy formula (20) as

$$\begin{aligned} p^* &= -\frac{\sigma_{11}^3}{\varepsilon_{11}} \frac{\partial}{\partial V}(N\varepsilon_x A^*)\Big|_{T,\{x_a\}}, \\ \mu_a^* &= \frac{1}{N\varepsilon_{11}} \frac{\partial}{\partial x_a}(N\varepsilon_x A^*)\Big|_{T,V,\{\check{x}_a\}}. \end{aligned} \tag{29}$$

Ref. [14] serves as a guide for the calculation of μ_a^* for LJ binary mixtures, and contains the LJ contributions to the free energy and pressure derived from a well founded equation of state.

Throughout this section and in the related figures we use the reduced units $T^* = kT/\varepsilon_{11}$, $\rho^* = \rho\sigma_x^3$, $d_a^{*2} = {d_a}^2/\sigma_{11}^3\varepsilon_{11}$ and $E_{\rm ext}^{*2} = {E_{\rm ext}}^2\sigma_{11}^3/\varepsilon_{11}$.

A. Vapor–liquid equilibrium

We have performed extensive vapor–liquid equilibrium calculations for a binary STM fluid in the vdW1f approximation with size and energy parameter ratios $\sigma_{22}/\sigma_{11} = 1.0$ and $\varepsilon_{22}/\varepsilon_{11} = 0.5$, respectively, at reduced temperature $T^* = 1.0$. Although the given choice of parameters seems to be *ad hoc*, our findings remains generally valid for their slight modifications (more on this later). The emphasis is on the structural change in equilibrium due to the interaction of the applied electric field with the dipole moments.

The critical data are $p^{c*} = 0.169$, $\rho^{c*} = 0.439$ and $x_1^c = 0.458$ for the dipole moments, $d_i^* = 0$. Table II shows the critical point 'wandering' caused by changes in the dipole moments or field strength. Three possiblities can be distinguished depending on which component of the mixture has a dipole moment: only the first, the second or both. In all cases there is an $E_{\rm ext}^{*2}$ value above which the vapor–liquid critical point cannot be found, and surprisingly enough the reasons—discussed below—are quite different (see Table II and Figs. 1–7).

(a) Case $d_2^{*2} = 0.0$. Table II shows that with zero applied field the reduced critical pressure p^{c*} and density ρ^{c*} clearly get higher and higher with increasing dipole moment d_1^{*2}. The mole fraction x_1^c increases in a less determined manner. For a given d_1^{*2} all of the critical data strongly increase when the electric field is turned on. One can find for each d_1^{*2} a maximal

$E^{*2}_{\rm ext}$ above which there is no vapor–liquid critical point, i.e. the contour of the two-phase region is open at the top. In advance, we were expecting the closed phase envelope to persist (although distorted in some way, of course), and the much more significant effect encouraged us to examine the equilibrium diagrams for higher pressures more closely. We have found that *above a lower critical solution pressure (LCSP) there are two partially miscible fluid phases, one of which is rich in the polar component.* Figure 1 displays the logarithm of the equilibrium pressure as a function of x_1, while Fig. 2 shows the same pressure as a function of ρ^* for various field strengths in case of $d_1^{*2} = 0.5$. For $E^{*2}_{\rm ext} = 0.075$ it is explicitly shown that well above the closed vapor–liquid phase boundary curve two fluid phases have been formed. The fluid–fluid critical point is characterised by the LCSP $p^* = 3.845$ and $\rho^* = 0.914$, $x_1 = 0.647$. Repeated small increases in the field strength decrease considerably the LCSP while the vapor–liquid critical pressure increases. Finally, the phase boundary curves fuse at the quadruple point:

$E^{*2}_{\rm ext}$	p^*	ρ^*	x_1
0.086496	1.1269	0.7833	0.6727

(30)

For even higher field strengths only the two fluid phases are presented.

The strong effect found for a moderately high electric field seems to be intimately related to the LJ parameters and dipole moments chosen. A small deviation in the ratio σ_{22}/σ_{11} from the unity does not alter much the phase equilibrium in contrast to the energy parameter ratio. The mixture shown in Fig. 1 has $\varepsilon_{22}/\varepsilon_{11} = 0.5$. The change to 0.6 results in the curves displayed in Fig. 3, which differ considerably from the preceding ones. Not so in their shapes (consider the logarithmic scale in Fig. 1) but instead in the field strength of the quadruple point. That is $E^{*2}_{\rm ext} = 0.0865$ approximately for the former system and 0.112

for the latter one. Moreover, let us point out that the 'effective' reduced dipole moment and field strength (defined in terms of σ_x and ε_x) may be higher, e.g. ${d_1}^2/\sigma_x^3\varepsilon_x = 0.612$ and $E_{\text{ext}}^2\sigma_x^3/\varepsilon_x = 0.1058$, respectively, in the quadruple point (30). Summing up, we believe that the large discrepancies in the energy parameters and the dipole moments of the two fluid components result as a cumulative effect in the appearance of the new fluid phases in presence of a sufficiently strong electric field.

(b) Case $d_1^{*2} = 0.0$. With increasing d_2^{*2} the critical pressure decreases as well as the critical density and the mole fraction, likewise in case of a given d_2^{*2} with increasing electric field strength. The mixture behaves exactly opposite to the system described above. Beyond that *the mixture shows positive azeotropy above a critical* E_{ext}^{*2} *value.* Fig. 4 proves that an azeotropic point occurs for the system under study with dipole moments $d_1^{*2} = 0.0$, $d_2^{*2} = 1.0$ provided that E_{ext}^{*2} is nearly 0.020 or higher. We note that a binary mixture is said to be at an azeotropic point if the corresponding mole fractions of the two phases become identical ($x_1' = x_1''$) without the densities being equal [8]. For the two azeotropic points of the system displayed in Fig. 4 the mixture parameters are

E_{ext}^{*2}	p^*	ρ'^*	ρ''^*	x_1
0.020	0.117	0.234	0.467	0.192
0.025	0.107	0.193	0.518	0.249

(31)

The pressure of the azeotrope decreases with increasing field strength, while the mole fraction increases, as well as the difference between the densities of the coexisting phases. Studying the variation of p^* in terms of ρ^* interesting *U-turns* occur at the azeotropic densities (see Fig. 5), for the equilibrium pressure is maximal at the azeotropic point.

(c) Case $d_1^{*2} = d_2^{*2}$. The dipole moments are set to be equal for simplicity, but the results

in general remain unchanged in case of a less polar first component and a more polar second one. The most remarkable feature of the mixture is that the critical mole fraction x_1^c of the first component diminishes rapidly with increasing field strength. The x_1^c required to be nearly zero for a sufficiently high $E_{\rm ext}^{*2}$ above which there is no vapor–liquid critical point (see the dotted lines in Figs. 6 and 7).

It is generally valid that the vapor pressure of a pure polar fluid decreases with increasing field strength. In all binary mixtures studied in this paper the first fluid component is the less volatile one, so its vapor pressure p_1^v is lower than the vapor pressure p_2^v of the second component. The vaporization and condensation pressures as functions of x_1 raise monotonically starting from p_1^v at $x_1 = 1.0$ and reaching p_2^v at $x_1 = 0.0$, or the vaporization and condensation curves meat at the critical point provided that the critical pressure p^c exceeds p_2^v. It is concluded from this case (c) that a dipolar fluid mixture in increasing electric field can on the whole behave like it was cooled. The electric field decreases the molecular disorder.

B. Liquid–liquid equilibrium

It is well known (see e.g. [18]) about binary LJ fluids that a suitable deviation measured by a parameter ξ from the Berthelot combining rule

$$\varepsilon_{12} = \xi\sqrt{\varepsilon_{11}\varepsilon_{22}} \tag{32}$$

brings in two partially miscible liquid phases bounded below by a LCSP. Now we study the liquid–liquid equilibrium in an electric field. The effect of a similar change

$$\sigma_{12} = \eta \frac{\sigma_{11} + \sigma_{22}}{2} \tag{33}$$

in the Lorentz rule will be treated in the next section. In the following examples we set $\xi = 0.75$ and $\sigma_{22}/\sigma_{11} = 0.8$, $\varepsilon_{22}/\varepsilon_{11} = 1.0$, $T^* = 1.15$.

a) Case $d_1^{*2} = 1.0$, $d_2^{*2} = 0.0$. Fig. 8 shows that with increasing field strength the LCSP decreases, and for a given pressure the region of liquid–liquid coexistence gets wider and wider. Furthermore, a sufficiently strong electric field fuses the liquid–liquid and vapor–liquid phase envelopes.

b) Case $d_1^{*2} = d_2^{*2} = 0.5$. In contrast with the preceding example for this choice of the dipole moments the regions of liquid–liquid and vapor–liquid coexistence intersect *without* any electric field (see Fig. 9). The effect of the electric field is similar to the former case, i.e. the increasing field strength enlarges the two-phase region.

c) It is worth noting that an alteration of the energy parameter ratio may weaken the effect of the dipole–dipole interaction on the two-phase properties. E.g. in Fig. 10 we set $\varepsilon_{11}/\varepsilon_{22} = 0.75$ and despite the higher dipole moments $d_1^{*2} = d_2^{*2} = 1.0$ the two-phase regions are isolated for zero or weak applied electric field, in contrast to the preceding case.

C. Chlorodifluoromethane + difluoromethane

The hidro(chloro)fluorocarbons (HCFC/HFC) serve [24] as potential alternatives for the halogenated chlorofluorocarbons to make ozone friendly propellants, refrigerants, solvents, etc. Extensive experimental and theoretical investigations have been started recently to

determine, among others, the thermodynamical properties, esp. vapor–liquid equilibria of HCFC/HFC binary mixtures. (See [24] and the referencies therein.) In Ref. [24] these mixtures were considered as dipolar ones, and Gibbs ensemble Monte Carlo (GEMC) simulations were performed with an effective STM potential model. The effective potential parameters ε, σ and $d^*_{\rm eff}$ for chlorodifluoromethane ($CHClF_2$) and difluoromethane (CH_2F_2), hereinafter referred to as R22 and R32, respectively, can be found in Table III. R32 seems [25] to be a possible compound of refrigerant mixtures, however, during the manufacturing process of R32 a certain amount of R22 is also produced, which has a considerably higher boiling point and therefore should be removed. An applied electric field may help—at least from a merely theoretical viewpoint—in the inevitable purification process. To put this idea on a sound basis, let us discuss the vapor–liquid equilibria curves (shown in Fig. 11) of the R22+R32 mixture taken at $T = 283.15$ K in various electric fields. In our calculations the free energy expression (20) and the potential parameters given in Table III were used, except that the reduced dipole moments $d^*_{\rm eff}$ taken from [24] were changed to d^*. This slight modification of the dipole moments was arose from a simple fitting to the experimentally determined [25] vapor pressures. In Fig. 11 solid lines refer to the case of zero applied field, and small squares represent the experimental data [25]. The fairly good agreement in the whole range of mole fractions proves the validity of the perturbation theory and the Lorentz–Berthelot combining rules applied here to describe the interaction between unlike particles. It should be noted that—in correspondence with the results published in Ref. [24]—for the mixture R22+R32 the introduction of a coefficient $\xi = 0.993$ in the Berthelot rule (32) was needed. As it can be seen in Fig. 11 and Table IV a sufficiently high—but experimentally accessible—electric field decreases the vapor pressures of pure compounds and significantly alter the R22 content of the two phases in vapor–liquid equilibrium at a given pressure.

D. Acetonitrile + methanol

The thermodynamic properties of acetonitrile and methanol—two important solvents of the chemical industry—can be well approximated [26] by the STM potential model, and their mixture shows [8] a characteristic positive azeotrope at room temperature. It is an interesting question to ask whether a strong electric field may end the azeotropy? To answer this question we determine the shifts in the vapor pressures and in the azeotropic point caused by an applied electric field. First of all, STM potential parameters are needed which we have taken from [26] (see Table V). However, the reduced dipole moments $d^*_{\rm eff}$ determined in [26] have to be modified considerably (cf. $d^*_{\rm eff}$ and d^* in Table V) to obtain the experimentally known vapor pressures of the pure compounds—a possible drawback of the method presented in [26]. A minor change in the Lorentz rule is also needed. We introduce the $\eta = 1.011$ coefficient in Eq. (33) to get the azeotropic point correctly. Fig. 12 shows our results for the acetonitrile+methanol mixture at $T = 333.46$ K. The solid line represents the case of zero electric field, and small squares indicate the corresponding experimental data [27]. The agreement is remarkable, considering the highly nontrivial shapes of the phase boundary curves. Small stars in Fig. 12 refer to GEMC simulations [28] based on *ab initio* pair potentials. In Ref. [28] the interaction between unlike molecules were determined separately without using any combining rules, and the phase boundary curves were found to be in good agreement with experiments [27]. However, for the case under study Fig. 12 proves the slight superiority of the perturbation theory applied in this paper.

In Fig. 12 the dashed and dotted lines present the perturbative effect of an applied electric field with different field strengths. The numerical results concerning the shifts in vapor pressures and in the azeotropic point are collected in Table VI. We have found that

an experimentally accessible field strength does not put an end to the azeotropic behavior of the mixture at or near the examined temperature.

IV. CONCLUSIONS

In this study we have proposed a theoretical model to incorporate the perturbative effect of an external electric field into the thermodynamics of dipolar fluid mixtures. We found a free energy expression (20) for binary STM fluids, which is valid up to third order in the perturbation expansion. The dielectric constant was calculated, and the result (22) was found to be a generalization of a formula [12, 20] widely accepted in case of dipolar hard sphere fluids up to moderately high dipole moments.

In Sec. III we have used our theory to calculate vapor–liquid and liquid–liquid equilibria in four cases. (A) In an example it has been demonstrated that a sufficiently high electric field may change considerably the shape of the vaporization and condensation curves, even a critical point may disappear and an azeotropic point may appear. For a careful choice of STM fluid parameters a strong electric field can separate the molecules into two partially miscible fluid phases, one of which is rich in the more polar molecules (see Fig. 1). The sufficient field strength seems to be experimentally unattainable, but it would be interesting to prove these results by MC simulations. (B) The liquid–liquid equilibrium also shows changes in an external field. The LCSP decreases with increasing field strength, and the two-phase region gets wider. (C) We have studied the mixture chlorodifluoromethane+difluoromethane at $T = 283.15$ K to investigate the role an applied electric field may play during the separation process of these two promising refrigerant compounds. We have concluded that the field effect turns to be important at field strengths as high as $5 \cdot 10^6$ V/m (see Fig. 11 and Table IV). (D) Similarly, in case of an acetonitrile+methanol mixture taken at $T = 333.46$ K

the considerable shifts in the vapor pressures or in the azeotropic point appear above a $2 \cdot 10^6$ V/m field strength, approximately (see Fig. 12 and Table VI).

Acknowledgments

The research was supported in part by the Hungarian National research Fund (OTKA-K61314). We are very grateful to S. I. Sandler for sending the paper [28] to us.

APPENDIX: THE ALGEBRAIC METHOD

In this Appendix a short summary of Ruelle's algebraic method [11, 12] extended [13] to fluid mixtures is given. The stress is laid on the free energy expression in presence of a perturbing field.

Consider a fluid mixture composed of K species of particles and described in the canonical ensemble. The potential energy of the refence system is of the form

$$U^0 = \sum_{i<j} u^0(ij). \tag{A.1}$$

Here and in the following i stands for $(\mathbf{r}_i, \omega_i, a_i)$ and $a_i \in \{1, \ldots, K\}$. Let the perturbation caused by an external field interacting with the particles be described by the potential $u^1(i)$. The configurational integral of the reference mixture reads

$$Z_N^0 = \int \mathrm{d}\mathbf{r}^N \mathrm{d}\omega^N e^{-\beta U^0}, \tag{A.2}$$

where N is the number of particles, $\mathrm{d}\mathbf{r}^N = \mathrm{d}\mathbf{r}_1 \cdots \mathrm{d}\mathbf{r}_N$ and $\beta = 1/kT$. The same integral

for the perturbed system is

$$\begin{aligned} Z_N &= \int \mathrm{d}\mathbf{r}^N \mathrm{d}\omega^N e^{-\beta U^0} \exp\big(-\beta \sum_i u^1(i)\big) \\ &= \int \mathrm{d}\mathbf{r}^N \mathrm{d}\omega^N e^{-\beta U^0} \prod_i (f_{\mathrm{M}}(i)+1) \\ &= \int \mathrm{d}\mathbf{r}^N \mathrm{d}\omega^N e^{-\beta U^0} \big(1+\sum_{n=1}^{N} \Phi_n(1\ldots N)\big). \end{aligned} \tag{A.3}$$

Here the Mayer function $f_{\mathrm{M}}(i) = (e^{-\beta u^1(i)} - 1)$ is introduced, and

$$\Phi_n(1\ldots N) = \sum_{1\le i_1<\ldots<i_n\le N} f_{\mathrm{M}}(i_1)\cdots f_{\mathrm{M}}(i_n). \tag{A.4}$$

Our goal is to expand the free energy

$$A = A^0 - \frac{1}{\beta}\ln\frac{Z_N}{Z_N^0} \tag{A.5}$$

of the perturbed fluid mixture in power series form. To this end the algebraic method is used, and we express the fraction Z_N/Z_N^0 in exponential form [see Eqs. (A.12) and (A.13) later]. First of all, we prove the following lemma.

LEMMA. Let $f(ijk)$ be a function which does not depend on the order of its arguments i, j, k, and let $f(ijk)$ be zero whenever any two of its arguments coincide. Then

$$\sum_{i,j,k=1}^{N} \int \mathrm{d}\mathbf{r}^3 \mathrm{d}\omega^3 f(ijk) = 3! \sum_{1\le i<j<k\le N} \int \mathrm{d}\mathbf{r}^3 \mathrm{d}\omega^3 f(ijk).$$

Proof. One can perform the following substitutions inside the multiple integral:

$$\sum_{i,j,k=1}^{N} f(ijk) \Rightarrow \sum_{k} \Big(\sum_{i<j} + \sum_{j<i} \Big) f(ijk) \Rightarrow 2 \sum_{k} \sum_{i<j} f(ijk)$$
$$\Rightarrow 2 \Big(\sum_{k<i<j} + \sum_{i<k<j} + \sum_{i<j<k} \Big) f(ijk) \Rightarrow 3! \sum_{i<j<k} f(ijk).$$

Clearly, one can extend the defining equation (A.4) of Φ_n in accordance with the Lemma. The one-particle correlation function $g^0(i) = g^0(\mathbf{r}_i, \omega_i, a_i)$ of the reference mixture is defined by

$$g^0(1) \frac{\rho_{a_1}}{\Omega_{a_1}} = N_{a_1} \frac{1}{Z_N^0} \int \mathrm{d}\mathbf{r}^{N-1} \mathrm{d}\omega^{N-1} e^{-\beta U^0}, \tag{A.6}$$

where $\rho_{a_1} = \rho x_{a_1}$, and $\Omega_{a_1} = 4\pi$ for linear molecules and $8\pi^2$ for nonlinear ones. The reference pair correlation function $g^0(ij)$ can be read from

$$g^0(12) \frac{\rho_{a_1} \rho_{a_2}}{\Omega_{a_1} \Omega_{a_2}} = N_{a_1} (N_{a_2} - \delta_{a_1 a_2})$$
$$\times \frac{1}{Z_N^0} \int \mathrm{d}\mathbf{r}^{N-2} \mathrm{d}\omega^{N-2} e^{-\beta U^0}, \tag{A.7}$$

and similar expressions are valid for the higher order correlation functions. With these notations and the Lemma in hand the summands in the integral (A.3) can be written in a more suitable form for later use. The first term (divided by Z_N^0) will be

$$\frac{1}{Z_N^0} \int \mathrm{d}\mathbf{r}^N \mathrm{d}\omega^N e^{-\beta U^0} \Phi_1(1 \ldots N)$$
$$= \frac{1}{Z_N^0} \int \mathrm{d}\mathbf{r}_1 \mathrm{d}\omega_1 \sum_{a_1=1}^{K} N_{a_1} f_{\mathrm{M}}(1) \int \mathrm{d}\mathbf{r}^{N-1} \mathrm{d}\omega^{N-1} e^{-\beta U^0}$$
$$= \sum_{a_1} \int \mathrm{d}\mathbf{r}_1 \mathrm{d}\omega_1 \frac{\rho_{a_1}}{\Omega_{a_1}} g^0(1) f_{\mathrm{M}}(1). \tag{A.8}$$

Here we have made use of the fact that the form of the Mayer function $f_{\mathrm{M}}(i)$ is the same for particles of the same type. The second summand of (A.3) can be written in the following form:

$$\begin{aligned}
&\frac{1}{Z_N^0}\int \mathrm{d}\mathbf{r}^N \mathrm{d}\omega^N e^{-\beta U^0}\Phi_2(1\dots N)\\
&= \frac{1}{Z_N^0}\int \mathrm{d}\mathbf{r}^N \mathrm{d}\omega^N e^{-\beta U^0}\frac{1}{2}\sum_{i\neq j} f_{\mathrm{M}}(i)f_{\mathrm{M}}(j)\\
&= \frac{1}{Z_N^0}\int \mathrm{d}\mathbf{r}_1\mathrm{d}\mathbf{r}_2\mathrm{d}\omega_1\mathrm{d}\omega_2\frac{1}{2}\sum_{a_1,a_2=1}^{K} N_{a_1}(N_{a_2}-\delta_{a_1a_2})\\
&\times f_{\mathrm{M}}(1)f_{\mathrm{M}}(2)\int \mathrm{d}\mathbf{r}^{N-2}\mathrm{d}\omega^{N-2}e^{-\beta U^0}\\
&= \frac{1}{2}\sum_{a_1a_2}\int \mathrm{d}\mathbf{r}_1\mathrm{d}\mathbf{r}_2\mathrm{d}\omega_1\mathrm{d}\omega_2\frac{\rho_{a_1}\rho_{a_2}}{\Omega_{a_1}\Omega_{a_2}}g^0(12)f_{\mathrm{M}}(1)f_{\mathrm{M}}(2).
\end{aligned} \tag{A.9}$$

Finally, the nth term will be

$$\begin{aligned}
&\frac{1}{Z_N^0}\int \mathrm{d}\mathbf{r}^N \mathrm{d}\omega^N e^{-\beta U^0}\Phi_n(1\dots N)\\
&= \frac{1}{n!}\sum_{a_1\dots a_n}\int \mathrm{d}\mathbf{r}^n \mathrm{d}\omega^n g^0(1\dots n)\prod_{k=1}^{n}\frac{\rho_{a_k}}{\Omega_{a_k}}f_{\mathrm{M}}(k).
\end{aligned} \tag{A.10}$$

Substituting (A.8–A.10) into (A.3) we get

$$\frac{Z_N}{Z_N^0} = 1+\sum_{n=1}^{N}\frac{1}{n!}\sum_{a_1\dots a_n}\int \mathrm{d}\mathbf{r}^n \mathrm{d}\omega^n g^0(1\dots n)\prod_{k=1}^{n}\frac{\rho_{a_k}}{\Omega_{a_k}}f_{\mathrm{M}}(k).$$

Here $\rho_{a_k} = \rho x_{a_k}$ and $\Omega_{a_k} = 4\pi$ for linear molecules studied in this paper, so

$$\frac{Z_N}{Z_N^0} = 1 + \sum_{n=1}^{N} \frac{z^n}{n!} \sum_{a_1 \ldots a_n} \int \mathrm{d}\mathbf{r}^n \mathrm{d}\omega^n g^0(1 \ldots n) \prod_{k=1}^{n} x_{a_k} f_{\mathrm{M}}(k), \tag{A.11}$$

where $z = \rho/4\pi$.

Now let us consider the thermodynamic limit $N \to \infty$. In this limiting case

$$\frac{Z_N}{Z_N^0} \to p(z) = \sum_{n=0}^{\infty} \frac{z^n}{n!} p_n, \qquad z = \frac{\rho}{4\pi}, \tag{A.12}$$

with $p_0 = 1$, and

$$p_n = \sum_{a_1 \ldots a_n} \int \mathrm{d}\mathbf{r}^n \mathrm{d}\omega^n g^0(1 \ldots n) \prod_{k=1}^{n} x_{a_k} f_{\mathrm{M}}(k)$$

for $n > 0$. Kalikmanov pointed out in Ref. [12] that the algebraic perturbation theory serves the fundamental expression

$$p(z) = \exp q(z) = \exp \left(\sum_{n=0}^{\infty} \frac{z^n}{n!} q_n \right), \tag{A.13}$$

where $q_0 = 0$, $q_1 = p_1$, $q_2 = p_2 - p_1^2$, $q_3 = p_3 - 3p_1p_2 + 2p_1^3$, etc. Eq. (A.13) together with (A.10) and (A.5) lead to the desired series expansion of the free energy:

$$A = A^0 - \frac{1}{\beta} \frac{\rho}{4\pi} q_1 - \frac{1}{2\beta} \left(\frac{\rho}{4\pi} \right)^2 q_2 - \ldots \tag{A.14}$$

The reference mixture is considered to be homogenous and isotropic, whereby $g^0(i) = 1$.

The first nontrivial terms of series $q(z)$ are

$$
\begin{aligned}
q_1 &= \sum_{a_1} \int \mathrm{d}\mathbf{r}_1 \mathrm{d}\omega_1 x_{a_1} f_{\mathrm{M}}(1) \\
q_2 &= \sum_{a_1 a_2} \int \mathrm{d}\mathbf{r}^2 \mathrm{d}\omega^2 (g^0(12) - 1) x_{a_1} x_{a_2} f_{\mathrm{M}}(1) f_{\mathrm{M}}(2) \\
q_3 &= \sum_{a_1 a_2 a_3} \int \mathrm{d}\mathbf{r}^3 \mathrm{d}\omega^3 (g^0(123) - 3g^0(23) + 2) \\
&\quad \times x_{a_1} x_{a_2} x_{a_3} f_{\mathrm{M}}(1) f_{\mathrm{M}}(2) f_{\mathrm{M}}(3).
\end{aligned} \tag{A.15}
$$

[1] D. Boda, I. Szalai and J. Liszi, J. Chem. Soc. Faraday Trans. **91**, 889 (1995).

[2] V. B. Warshavsky and X. C. Zeng, Phys. Rev. E **68** 051203 (2003).

[3] B. Groh and S. Dietrich, Phys. Rev. E **53** 2509 (1996).

[4] I. Szalai, K.-Y. Chan, Y. W. Tang, Molec. Phys. **101**, 1819 (2003).

[5] J. Hegseth and K. Amara, Phys. Rev. Lett. **93**, 057402 (2004).

[6] K. D. Blankenship, V. M. Shah, C. Tsouris, Sep. Sci. Tech. **34**, 1393 (1999).

[7] J.-P. Hansen and I. R. McDonald, *Theory of simple liquids*, 2nd Ed., Academic Press, New York (1986).

[8] J. S. Rowlinson, *Liquids and Liquid Mixtures*, 2nd Ed., Butterworth, London (1969).

[9] I. Szalai and S. Dietrich, Molec. Phys. **103**, 2873 (2005).

[10] W. R. Smith, Can. J. Phys. **52**, 2022 (1974).

[11] D. Ruelle, *Statistical Mechanics: Rigorous Results*, World Scientific, Singapore (1999).

[12] V. I. Kalikmanov, Phys. Rev. E **59**, 4085 (1999).

I. Szalai, K. Y. Chan and D. Henderson, Phys. Rev. E **E62**, 8846 (2000).

[13] G. Kronome, I. Szalai and J. Liszi, J. Chem. Phys. **116**, 2067 (2002).

[14] J. K. Johnson, J. A. Zollweg and K. E. Gubbins, Molec. Phys. **78**, 591 (1993).

[15] M. Luckas, K. Lucas, U. Deiters and K. E. Gubbins, Molec. Phys. **57**, 241 (1986).

[16] J. J. Nicolas, K. E. Gubbins, W. B. Strett and D. J. Tildesley, Molec. Phys. **37**, 1429 (1979).

[17] V. I. Harismiadis, N. K. Koutras, D. P. Tassios and A. Z. Panagiotopoulos, Fluid Phase Equilibria **65**, 1 (1991).

[18] A. M. Georgoulaki, I. V. Ntouros, D. P. Tassios and A. Z. Panagiotopoulos, Fluid Phase Equilibria **100**, 153 (1994).

[19] B. Groh and S. Dietrich, Phys. Rev. E **50**, 3814 (1994).

[20] A. Tani, D. Henderson, J. A. Barker and C. E. Hecht, Molec. Phys. **48**, 863 (1983).

[21] S. Goldman, Molec. Phys. **71**, 491 (1990).

[22] J. S. Høye and G. Stell, J. Chem. Phys. **63**, 5342 (1975).

[23] M. P. Allen and D. J. Tildesley, *Computer Simulation of Liquids*, Chapter 6., Clarendon, Oxford (2001).

[24] G. T. Gao, W. Wang and X. C. Zeng, Fluid Phase Equilibria **158–160**, 69 (1999).

[25] Y. W. Kang and K. Y. Chung, J. Chem. Eng. Data **41**, 443 (1996).

[26] M. E. van Leeuwen, Fluid Phase Equilibria **99**, 1 (1994).

[27] J. Gmehling, U. Onken and W. Arlt, *Vapor–Liquid Equilibrium Data Collection*, DECHEMA, Frankfurt, Germany (1977-onward).

[28] A. K. Sum, S. I. Sandler, R. Bukowski and K. Szalewicz, J. Chem. Phys. **116**, 7637 (2002).

List of Figures

Figure 1. Plots for the equilibrium pressure p^* on logarithmic scale against x_1 for a mixture ($\sigma_{22}/\sigma_{11} = 1.0$, $\varepsilon_{22}/\varepsilon_{11} = 0.5$, $T^* = 1.0$) in various electric fields with dipole moments $d_1^{*2} = 0.5$, $d_2^{*2} = 0.0$.

Figure 2. Plots for the equilibrium pressure p^* against ρ^* for the mixture in Fig. 1.

Figure 3. Plots for the equilibrium pressure p^* against x_1 for a mixture ($\sigma_{22}/\sigma_{11} = 1.0$, $\varepsilon_{22}/\varepsilon_{11} = 0.6$, $T^* = 1.0$) in various electric fields with dipole moments $d_1^{*2} = 0.5$, $d_2^{*2} = 0.0$.

Figure 4. Plots for the equilibrium pressure p^* against x_1 for a mixture ($\sigma_{22}/\sigma_{11} = 1.0$, $\varepsilon_{22}/\varepsilon_{11} = 0.5$, $T^* = 1.0$) in various electric fields with dipole moments $d_1^{*2} = 0.0$, $d_2^{*2} = 1.0$.

Figure 5. Plots for the equilibrium pressure p^* against ρ^* for the mixture in Fig. 4.

Figure 6. Plots for the equilibrium pressure p^* against x_1 for a mixture ($\sigma_{22}/\sigma_{11} = 1.0$, $\varepsilon_{22}/\varepsilon_{11} = 0.5$, $T^* = 1.0$) in various electric fields with dipole moments $d_1^{*2} = d_2^{*2} = 1.0$.

Figure 7. Plots for the equilibrium pressure p^* against ρ^* for the mixture in Fig. 6.

Figure 8. Plots for the equilibrium pressure p^* on the logarithmic scale against x_1 for a mixture ($\xi = 0.75$, $\sigma_{22}/\sigma_{11} = 0.8$, $\varepsilon_{22}/\varepsilon_{11} = 1.0$, $T^* = 1.15$) in various electric fields with dipole moments $d_1^{*2} = 1.0$, $d_2^{*2} = 0.0$.

Figure 9. Plots for the equilibrium pressure p^* on the logarithmic scale against x_1 for a mixture ($\xi = 0.75$, $\sigma_{22}/\sigma_{11} = 0.8$, $\varepsilon_{22}/\varepsilon_{11} = 1.0$, $T^* = 1.15$) in various electric fields with dipole moments $d_1^{*2} = d_2^{*2} = 0.5$.

Figure 10. Plots for the equilibrium pressure p^* on the logarithmic scale against x_1 for a mixture ($\xi = 0.75$, $\sigma_{22}/\sigma_{11} = 0.8$, $\varepsilon_{22}/\varepsilon_{11} = 0.75$, $T^* = 1.15$) in various electric fields with dipole moments $d_1^{*2} = d_2^{*2} = 1.0$.

Figure 11. Plots for the equilibrium pressure p (measured in bars) against the mole fraction x_1 of R22 for the mixture R22+R32 at $T = 283.15$ K in various electric fields.

Experimental data for $E_{\rm ext} = 0.0$ are taken from Ref. [25].

Figure 12. Plots for the equilibrium pressure p (measured in bars) against the mole fraction x_1 of acetonitrile for the mixture acetonitrile+methanol at $T = 333.46$ K in various electric fields. For the case of zero applied field some experimental data [27] and the results [28] of GEMC simulations with *ab initio* pair potentials are also presented.

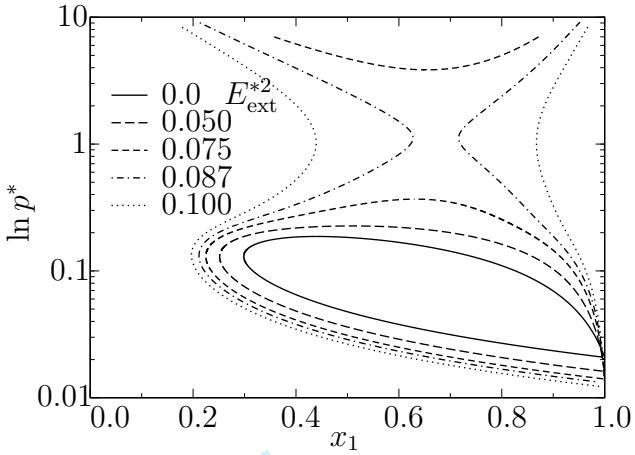

FIG. 1: Gábor and Szalai, J.Chem.Phys.

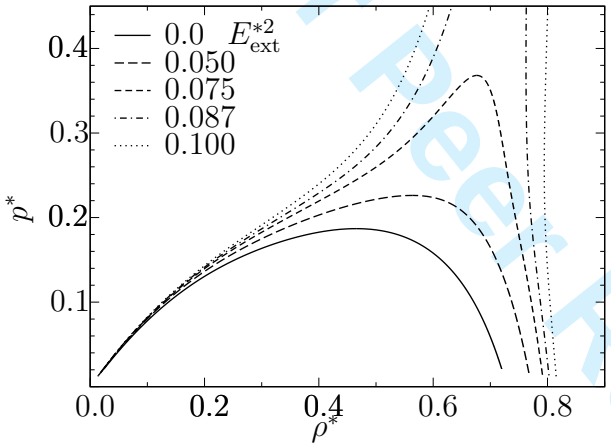

FIG. 2: Gábor and Szalai, J.Chem.Phys.

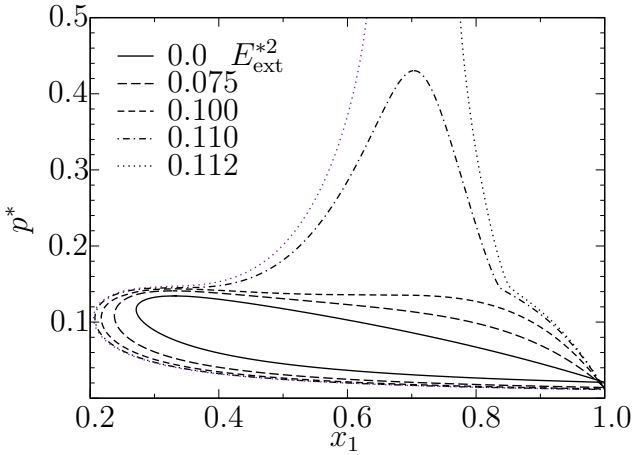

FIG. 3: Gábor and Szalai, J.Chem.Phys.

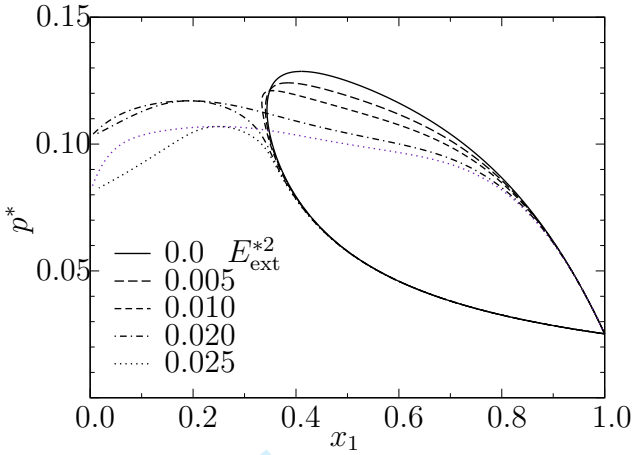

FIG. 4: Gábor and Szalai, J.Chem.Phys.

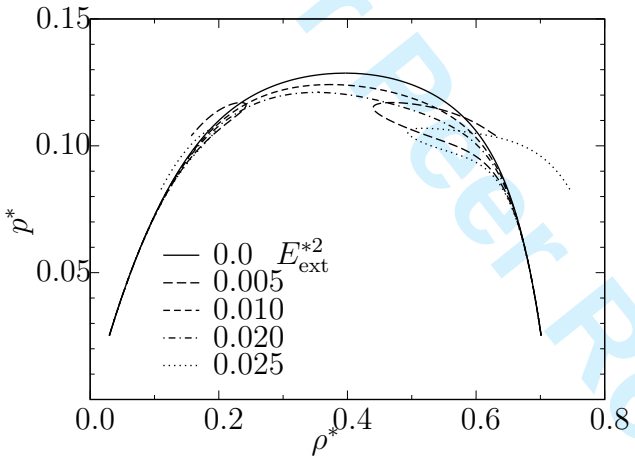

FIG. 5: Gábor and Szalai, J.Chem.Phys.

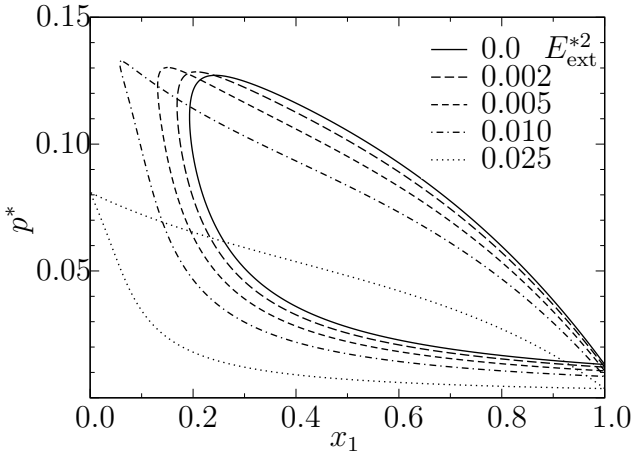

FIG. 6: Gábor and Szalai, J.Chem.Phys.

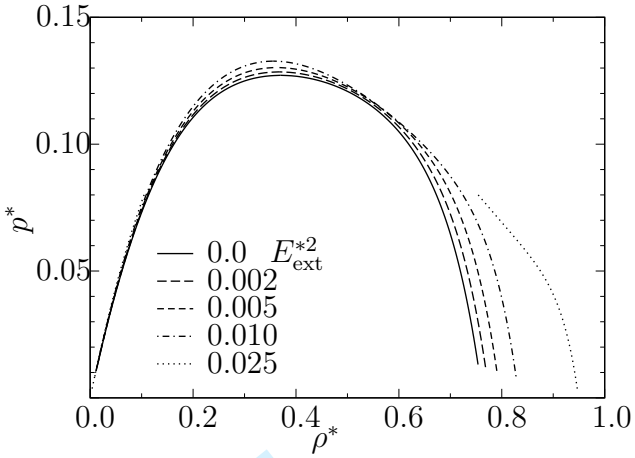

FIG. 7: Gábor and Szalai, J.Chem.Phys.

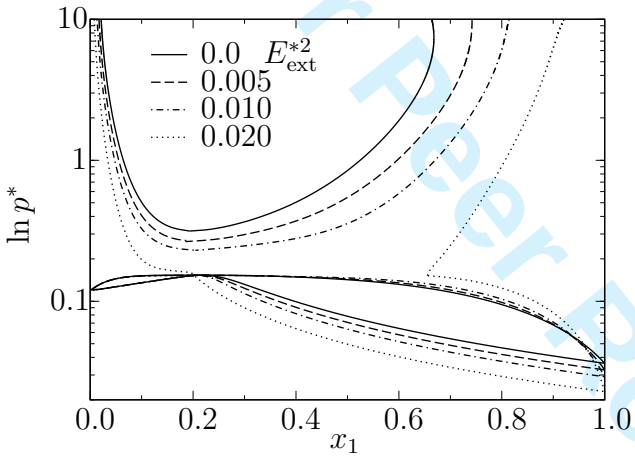

FIG. 8: Gábor and Szalai, J.Chem.Phys.

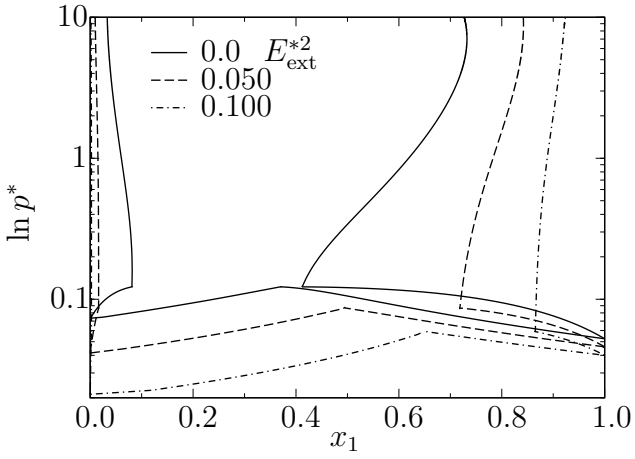

FIG. 9: Gábor and Szalai, J.Chem.Phys.

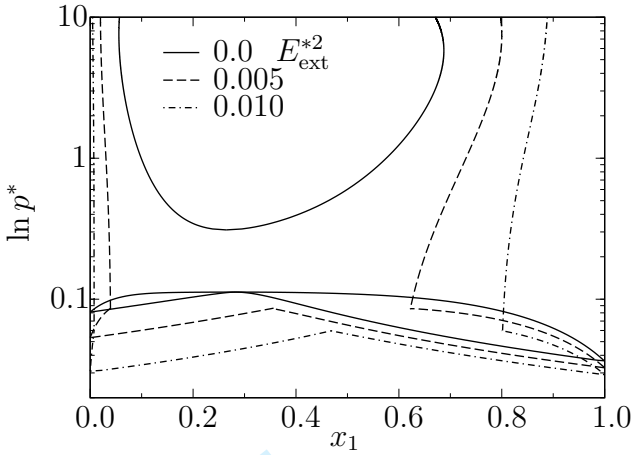

FIG. 10: Gábor and Szalai, J.Chem.Phys.

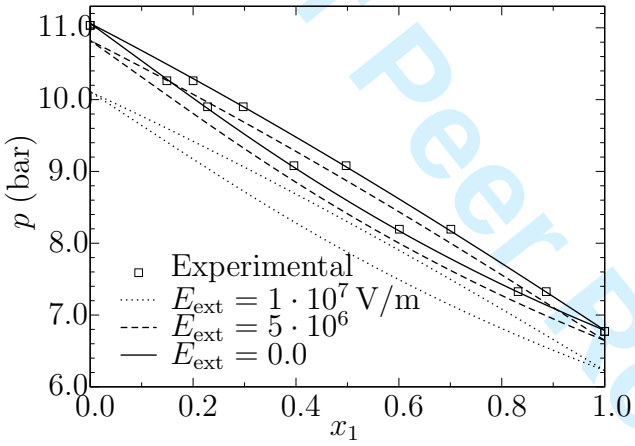

FIG. 11: Gábor and Szalai, J.Chem.Phys.

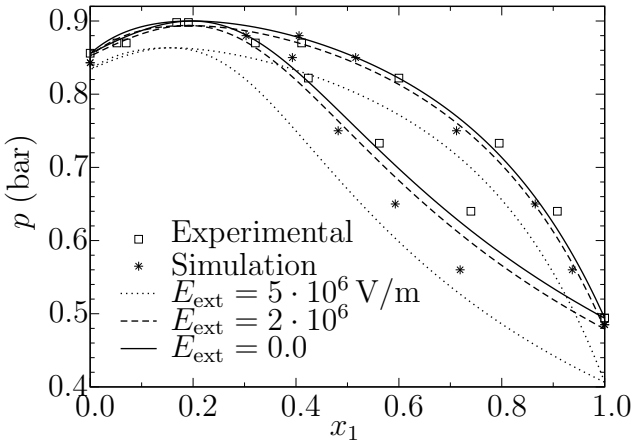

FIG. 12: Gábor and Szalai, J.Chem.Phys.

Tables

TABLE I: The matrix (b_{ij}) of the coefficients in Eq. (27).

19.07848434	−0.02206566	0.03267467	−0.43489042
24.11991429	−7.16957630	−2.46413554	2.48863015
−54.94579263	17.95946765	14.05731128	−19.26865259
26.48841930	−10.82856816	−17.29258662	29.21044620

TABLE II: Critical data of a binary STM fluid in the vdW1f approximation ($\sigma_{22}/\sigma_{11} = 1.0$, $\varepsilon_{22}/\varepsilon_{11} = 0.5$, $T^* = 1.0$) with various dipole moments and external field strengths. For each pair of dipole moments and field strength the reduced critical pressure p^{c*}, density ρ^{c*} and mole fraction x_1^c are given one under the other.

d_1^{*2}	d_2^{*2}	E_{ext}^{*2}						
		0.0	0.002	0.005	0.010	0.025	0.050	0.075
0.5	0.0	0.187	0.188	0.189	0.192	0.201	0.226	0.368
		0.465	0.467	0.471	0.477	0.501	0.563	0.676
		0.440	0.440	0.442	0.444	0.457	0.509	0.631
0.75	0.0	0.213	0.219	0.229	0.257			
		0.507	0.519	0.539	0.584	–[1]		
		0.439	0.447	0.462	0.504			
1.0	0.0	0.272	0.315	0.502				
		0.574	0.608	0.684	–[1]			
		0.462	0.490	0.557				
1.25	0.0	0.439	1.025					
		0.643	0.750	–[1]				
		0.471	0.523					
0.0	0.5	0.158	0.157	0.157	0.156	0.153	0.149	0.146
		0.433	0.428	0.427	0.426	0.421	0.415	0.406
		0.450	0.446	0.445	0.443	0.438	0.431	0.421
0.0	0.75	0.145	0.144	0.142	0.140	0.133	0.128	
		0.418	0.416	0.413	0.406	0.382	0.346	–[2]
		0.434	0.432	0.428	0.420	0.393	0.320	
0.0	1.0	0.129	0.127	0.124	0.121			
		0.396	0.387	0.373	0.356	–[2]		
		0.410	0.401	0.384	0.356			
0.5	0.5	0.159	0.159	0.160	0.161	0.162	0.164	0.164
		0.430	0.428	0.429	0.430	0.427	0.426	0.416
		0.396	0.390	0.383	0.371	0.332	0.273	0.210
0.75	0.75	0.145	0.146	0.147	0.148	0.150		
		0.410	0.410	0.408	0.403	0.388	–[3]	
		0.330	0.314	0.289	0.246	0.126		
1.0	1.0	0.127	0.129	0.130	0.133			
		0.370	0.367	0.362	0.353	–[3]		
		0.243	0.206	0.151	0.060			

TABLE III: Effective STM parameters quoted from [24]. Concerning the dipole moment d^* see the main text.

Compound		ε/k (K)	σ (Å)	d_{eff}^*	d^*
R22	$CHClF_2$	199.8	4.374	1.768	1.728
R32	CH_2F_2	163.1	3.900	2.098	2.051

TABLE IV: Shifts in the vapor pressures p^v_{R22} and p^v_{R22} of pure R22 and R32 compounds, respectively, in electric field E_{ext}.

E_{ext} (V/m)	0.0	$1 \cdot 10^6$	$2 \cdot 10^6$	$5 \cdot 10^6$	$1 \cdot 10^7$
p^v_{R22} (bar)	6.788	6.782	6.765	6.647	6.229
p^v_{R32} (bar)	11.056	11.049	11.020	10.820	10.106

TABLE V: STM potential parameters of acetonitrile and methanol [26]. Concerning the dipole moment d^* see the main text.

Compound		ε/k (K)	σ (Å)	d^*_{eff}	d^*
Acetonitrile	CH_3CN	175.7	4.284	2.838	2.783
Methanol	CH_3OH	359.0	3.803	1.036	1.516

TABLE VI: Shifts in the azeotropic pressure p^a and mole fraction x^a_1 of the mixture acetonitrile+methanol, and in the vapor pressures p^v_1 and p^v_2 of pure acetonitrile and ethanol, respectively, caused by the electric field E_{ext}.

E_{ext} (V/m)	0.0	$1 \cdot 10^6$	$2 \cdot 10^6$	$5 \cdot 10^6$
p^a (bar)	0.900	0.898	0.894	0.863
x^a_1	0.198	0.196	0.191	0.156
p^v_1 (bar)	0.494	0.490	0.479	0.407
p^v_2 (bar)	0.856	0.855	0.853	0.834